Journal of MATERIALS RESEARCH

Invited Paper
DOI:10.1557/s43578-024-01321-9

Is the field of organic thermoelectrics stuck?

Irene Brunetti[1,2,3], Aditya Dash[1], Dorothea Scheunemann[1], Martijn Kemerink[1,a)]

[1] Institute for Molecular Systems Engineering and Advanced Materials, Heidelberg University, Im Neuenheimer Feld 225, 69120 Heidelberg, Germany
[2] InnovationLab, Speyererstrasse 4, 69115 Heidelberg, Germany
[3] Light Technology Institute, Karlsruhe Institute of Technology, Engesserstrasse 13, 76131 Karlsruhe, Germany
[a)] Address all correspondence to this author. e-mail: martijn.kemerink@cam.uni-heidelberg.de

Received: 14 February 2024; accepted: 4 March 2024

With the rising popularity of organic thermoelectrics, the interest in doping strategies for organic semiconductors has increased strongly over the last decade. Here, we use aggregate data to discuss how far the approaches pursued till date have brought the community in terms of typical performance indicators for doped semiconductors in the context of thermoelectric applications. Surprisingly, despite the superlinear increase in the number of publications on the subject matter, the performance indicators show no clear upward trend in the same time range. In the second part, we discuss possible approaches to break this deadlock. A specifically promising approach, controlling the distribution of dopant atoms in the host material, is discussed in some quantitative detail by experiments and numerical simulations. We show that spontaneous modulation doping, that is, the spatial separation between static dopant ions and mobile charge carriers, leads to a dramatic conductivity increase at low dopant loading.

Introduction

The technological and societal relevance of inorganic semiconductors can be directly traced back to the possibility to change their electronic conductivity by doping. The doping can either be electrostatic in nature through the (reversible) application of gate voltages in transistor-type devices or by the (typically irreversible) incorporation of heteroatoms in the semiconductor crystal lattice. In that light, it is remarkable how little attention chemical doping of organic semiconductors has received during the booming interest in these materials after the Nobel Prize for Chemistry was awarded to Heeger, MacDiarmid and Shirakawa in the year 2000 for the discovery and development of conductive, that is, chemically doped polymers. The data in Fig. 1 show a relatively modest baseline below 200 publications per year (black symbols), with a significant upswing around 2013. As shown in Fig. S1 in the Supporting Information, electrostatic (gate) doping of OSC shows a much stronger publication activity with an almost linear increase in publications/year, starting from 2002 and peaking at ~ 2000 publications/year in 2017.

A closer inspection of Fig. 1 allows some further observations. First, the sum of the publication counts for the organic thermoelectrics (OTE, red symbols), mixed electronic-ionic conductors (blue), and organic diodes and organic photovoltaics (OPV, green) roughly equals the total count for doped organics, cf. thin black line and black symbols. While the fraction of diode and OPV papers to the sum drops from well above 50% prior to 2010 to currently less than 20%, the fraction of OTE papers increases from around 30% before 2010 to currently ~ 70%. This allows the conclusion that the increasing interest in doped OSC is mainly driven by the increasing activity on organic thermoelectrics. We take this as a justification to use the common metrics for OTE, conductivity σ, Seebeck coefficient S and the power factor $PF = S^2\sigma$ as Figures of Merit (FoM) for doped OSC. Of course, depending on the application, other FoM might be equally or even more important—in the following, we will, for instance, ignore factors like stability, ion diffusivity, etc. Although the key FoM of thermoelectrics is the dimensionless number $zT = PF/\kappa T$, with κ the thermal conductivity, we will limit the discussion thereof by lack of data points. The latter is associated with the difficulty to reliably measure thermal conductivity in the thin-film geometries that are common in the field, that is, in the same direction as the PF measurement, parallel to the plane of the substrate.

We further note that the interest in doped OSCs seems to be broadening due to the development of mixed electronic-ionic conductors (green symbols), which are receiving increased attention for, among others, sensing applications

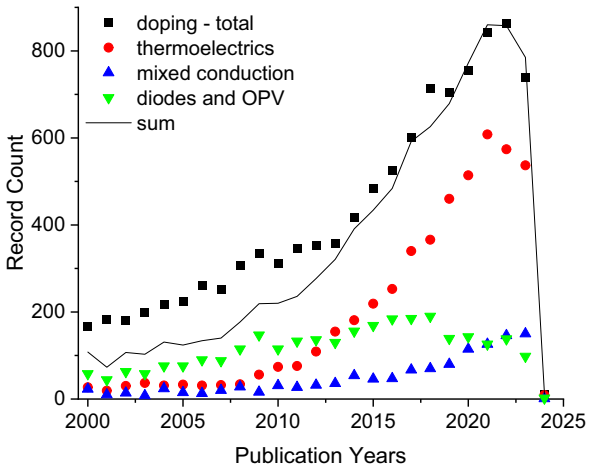

Figure 1: Number of publications on the indicated topic (see legend) vs. publication year. Data obtained from the Web of Science Core Collection on 16.01.2024. All queries are confined to organic materials, excluding, where needed, (hybrid) perovskites. The queries used are given in the Supporting Information, Section 1. The thin line is the sum of the thermoelectrics, mixed conduction, and diodes and OPV categories.

in biological systems, including interfacing with neural systems [1]. The dominant contribution to the 'diodes and OPV' category are interfacial layers that are used in organic solar cells, and (light-emitting) diodes in general to improve contact properties, including charge selectivity, built-in field and injection (diodes) and extraction (OPV) [2, 3].

Analysis of FoM over time

In the International Training Network on Hybrid and Organic Thermoelectrics (HORATES, Horizon 2020 MSC Action), we built up an open-access database with representative thermoelectric data for p- and n-type materials from the available literature [4]. Fig. 2 shows the key thermoelectric FoM from this database versus year of publication. Surprisingly, and worryingly, neither the conductivity nor the power factor of p-type materials shows any sign of an upward trend with time. Rather, the increasing number of publications in later years has led to a higher number of entries at lower FoM. The latter in itself is not problematic, as producing insight and understanding is an important goal of science that typically does not combine well with producing records. At the same time, in a field where applications are generally considered to be so near, one would hope that the provided insights and design rules condense in a gradual increase in FoM. Such a clearly increasing upward trend has, for example, been evidenced in the related field of organic photovoltaics. Here, the power conversion efficiency of both binary and ternary systems shows such a trend, reflecting an increased collective understanding and the existence of practical design rules, even if details are still debated [5].

In contrast to σ and PF, the Seebeck coefficient of p-type materials does show an upward trend. Unfortunately, for most applications, S is not the key FoM. Particularly, the lack of corresponding increase in PF suggests that the increase in S

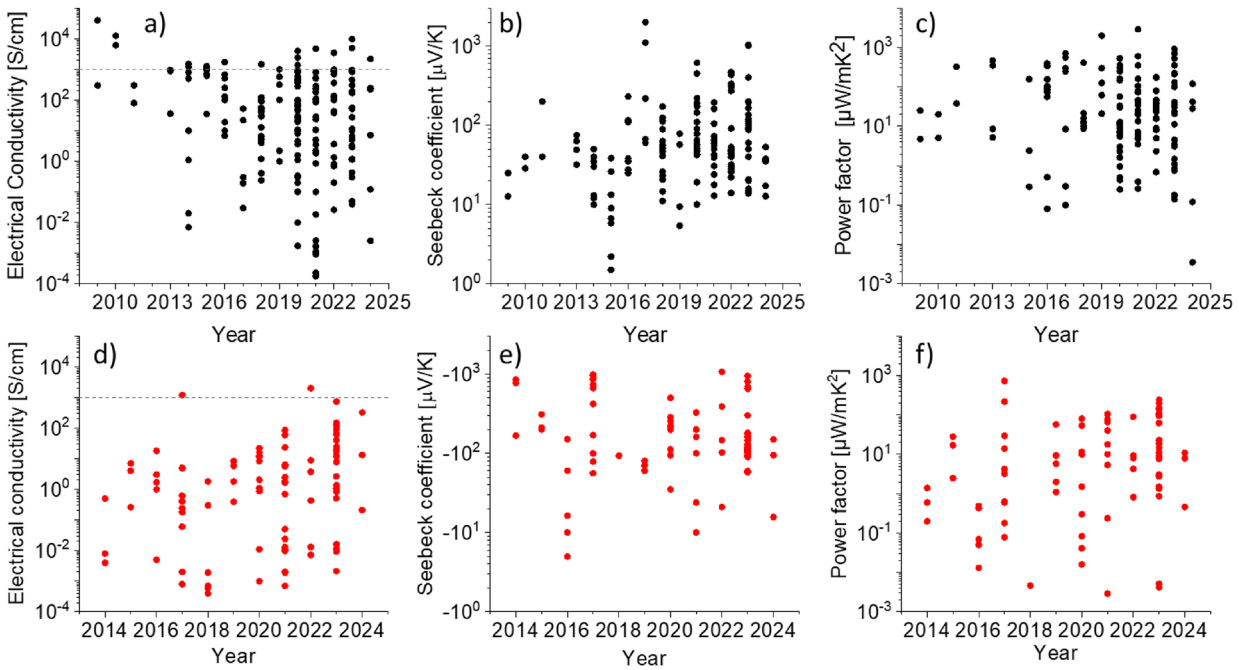

Figure 2: Figures of Merit for thin film-doped organic semiconductors collected from literature vs. year of publication, focusing on thermoelectric parameters. Upper (a–c) and lower (d–f) rows are for p-type and n-type materials, respectively. A table with the used literature references can be found in the SI, Sect. 2.

comes at the cost of a reduced σ due to the well-known trade-off between conductivity and Seebeck coefficient [6, 7]. As suggested by the opposing trends in σ and S in [Fig. 2(a, b)], plotting these parameters against each other in Fig. S2 shows that, at the aggregate level, this trade-off is indeed still active, despite many individual papers demonstrating the breaking thereof: although not as pronounced as when the doping level is varied for a single material, the trends $S \propto \sigma^{-1/4}$ and hence $PF \propto \sigma^{1/2}$ are clearly observable in Fig. S2.

For n-type materials, the conductivity and power factor of typical best materials are about an order of magnitude lower than for p-type, cf. [Figs. 2(a–d) and (c–f)]. When plotted as PF vs σ (Fig. S2), n- and p-type materials are on the same trend line. This suggests that the limiting factor for TE performance for n-types is indeed mostly the conductivity and not the Seebeck coefficient and that their charge and energy transport are—unsurprisingly—governed by the same mechanisms. Accordingly, the somewhat higher S values for n-types in [Fig. 2(e)] are to be understood as a reflection of their lower conductivity. At the same time, one might, with a willing eye, identify an upward trend in the conductivity and power factor that could indicate a catching up with p-type materials that have traditionally dominated the field of organic semiconductors, mostly for reasons of stability.

In SI Fig. S3, a similar analysis as above of zT and the thermal conductivity κ of OTEG materials is made. Despite the limited number of data points, the absence of (upward) trends for ZT is consistent with the above. Interestingly, the near independence of κ on electrical conductivity suggests strongly that $\kappa = \kappa_{latt} + \kappa_{el}$ is dominated by the lattice contribution κ_{latt}, as the electronic contribution κ_{el} would be expected to roughly follow the Wiedemann–Franz form $\kappa_{el} = LT\sigma$. Using the Sommerfeld value for the Lorenz number L, $L_0 = \frac{\pi^2}{3}\left(\frac{k_B}{q}\right)^2 = 2.45 \times 10^{-8}$ WΩ/K^2, leads to $\kappa_{el} \sim 7$ W/mK for a high but realistic conductivity of 10^4 S/cm and a temperature $T = 300$ K. This can only be reconciled with reported values of $\kappa \sim 1$ W/mK at similar or even higher conductivities by assuming that the actual Lorenz number of highly doped organic materials can be much below the Sommerfeld value for free electrons. Although some of us have argued that this, to some degree, might indeed be the case [8], this is clearly an important direction of future research.

Summarizing, the literature data discussed above indicate that the field of organic thermoelectrics and possibly the broader field of doped organic semiconductors is stuck when looking at the aggregate level and focusing on conductivity and other thermoelectric performance indicators. Of course, this does not do justice to important progress that has been reported in individual papers. To mention one specific result that might bring n-type materials to the p-type level as set by PEDOT-derivatives, Tang and coworkers recently reported the PEDOT-like side chain-free n-type polymer PBFDO that shows good ambient stability and a conductivity around 2000s/cm [9]. Although the Seebeck coefficient (– 21 μV/K) and power factor (90 μW/mK^2) are still modest and actually at the level of standard high-conductivity PEDOT:PSS, there might be significant room for improvement, both though post-processing and structural variation [10].

Mitigation of FoM-limiting factors

In order to identify directions to create an upswing in the FoM of doped OSC, it is worthwhile to draw an analogy with the situation in the field of organic photovoltaics (OPV) prior to the introduction of 'modern' non-fullerene acceptors (NFA). In the period 2011–2016 the record single OPV cell power conversion efficiency (PCE) was somewhat stuck between 10 and 12%, see SI Fig. S4 [11]. In contrast to the OTE community, the OPV community did, at the time, have a clear diagnose of what was wrong (poor spectral overlap, large voltage losses) [12–14] and accordingly could identify means to mitigate those problems [15]. For doped OSC, in contrast, there is no theory that is equivalent to the (extended) Shockley model for OPV that would allow us to identify sub-optimal performance in terms of σ, S, (and κ): we do not know how far these parameters, and accordingly PF and ZT can be realistically pushed. As such, the field urgently needs a predictive and universally applicable theory to understand where there is room for improvement.

In absence of such a theory—if such a theory is even possible—we can make a rough estimate of the conductivity that might be reached. Taking as an empirical upper limit for the charge carrier mobility a value for good single crystals, $\mu = 10$ cm^2/Vs and a charge carrier density that is equal to a typical (monomer) site density of $n = N_0 \sim 10^{21}$ cm^{-3} gives $\sigma = q\mu n \sim 10^3$ S/cm, which is not much below where to we are for p-type materials, cf. the dashed lines in [Fig. 2(a) and (d)]. Hence, getting to higher conductivities might be challenging, and one would rather have to look for improvement in the direction of beating the trade-off with S and possibly κ_{el} [8]. Likewise, the study of κ_{latt} is in its infancy and one may expect major improvement potential, for instance, in designing 'phonon-glass electron-crystal'-type systems [16].

Zooming in on the dopants used for the power factor data of p-type materials, Fig. S5 shows that the (higher PF-part of the) field is dominated by essentially three dopants: $FeCl_3$, F_nTCNQ ($n = 4, 6$), and Mo(tfd-X)$_3$ and that none of these significantly surpasses the values for the older PEDOT-derivatives. That situation is reminiscent of the pre-NFA times in OPV discussed above, where a limited set of fullerene derivatives was blended with 'any' available donor polymer. This suggests another direction for further optimization, in the form

of semiconductor/dopant combinations that are tailored to each other, as opposed to a one-size-fits-all approach. Another interesting aspect of Fig. S5 is the fact that also single-walled carbon nanotubes (SWNT), at least in the more application-relevant thin-film form, appear to be stuck at power factors slightly below 10^3 μW/mK^2, despite the intrinsically high mobilities in SWNT. Since the transport theory of doped and disordered nanotube networks is (even) less developed than for OSC, recent work by some of us highlighted significant similarities while simultaneously suggesting that *ZT* reaching or even exceeding unity might be possible [17].

Despite absence of the equivalent of a 'Shockley theory' for doped OSC, the current understanding within the community allows to identify a number of qualitative performance limiting factors. These are in order of relative importance as measured by the number of papers dedicated to each: (1) the active layer morphology, which may or may not be perturbed by incorporation of dopant molecules; (2) Coulomb scattering and charge carrier trapping by ionized dopants; and (3) bipolaron formation, with the notion that bipolarons are immobile or at least less mobile than single polarons. At the same time, the questions whether bipolarons are generally stable in chemically doped films and how they might be detected have not been univocally answered [18, 19]. It is not the purpose of this perspective to provide a review of the excellent work that has been done on these topics. Instead, we will briefly address some of the mitigation strategies that have been pursued and that, in our view might be pushed further to beat the status quo, for instance, by designing and synthesizing matching dopant-semiconductor pairs.

In general, it is well known that dopant molecules do not distribute randomly over the host material, but instead show a rich behavior of preferential positions and orientations, depending on the specific host–guest combination and relative concentrations, the host morphology (e.g., amorphous or ordered), and processing conditions (e.g., one-pot or sequential from solution or the vapor phase). Consensus seems to exist that host–guest systems where dopant incorporation leaves a preferentially dominant, well-ordered host phase intact, for instance, by intercalating in the alkyl side chains [20], are preferred [21]. However, experiences so far suggest that this alone is not sufficient to beat the 'typical best' results in Fig. 2. Instead, it seems one has to search for more subtle effects by, for example, upfront designing the efficiency of charge transfer [22], the screening of detrimental Coulomb interactions [16, 23], and/or avoiding the formation of bound bipolaron or hybrid states [19, 24].

An alternative and possibly generic direction that is reminiscent of the use of ternary blends in OPV is the use of blends of two semiconductors and one dopant [25–27]. Although the benefits in terms of power factor so far have not been as significant as the increases in PCE of ternary OPV [5], experimental results have shown the possibility to improve *PF* beyond the single-semiconductor value, although the mechanism are not always exactly clear [27, 28].

A third-generic direction that we want to highlight makes use of the fact that conjugated polymers are inherently anisotropic materials and that for thermoelectric applications only the properties in one direction, that of the charge and energy flow, matter; strategies to decouple these directions exist, but so far seem beyond practical application [29]. Various works have experimentally demonstrated an increase in *PF* and even a combined increase in σ and *S*, by mechanically aligning the polymer backbone [30–32]. In fact, Vijayakumar et al. achieved $PF = 2$ mW/mK^2 using this method, which is (one of) the highest values reported so far [33]. Current theoretical understanding suggests that indeed this method provides a universal way forward to improve already good thermoelectric performance, which sets it apart from other proposed design rules [34].

In the last part of this perspective, we build on the above and address two specific examples of (potential) design strategies in some quantitative detail. This list, which focusses on some effects of inhomogeneous dopant distributions, should by no means be considered as exhaustive.

Example 1: Spontaneous modulation doping

As discussed above, the high doping densities that are often necessary to maximize σ and *PF* for thermoelectric materials, adversely affect the conductivity [21]. A possible strategy to circumvent these drawbacks was recently introduced by Dash, Guchait, and coworkers for semi- and liquid-crystalline conjugated polymers [35]. This approach, which allows extremely efficient doping and thus high conductivity even at low dopant concentrations, is based on the spatial separation of dopant anions and mobile charge carriers. In inorganic semiconductor heterostructures, this concept is known as modulation doping and is used to fabricate high-mobility devices through elaborate top-down crystal growth techniques. For suitable polymer/dopant combinations, this process can occur spontaneously. The preconditions for this to work are a morphology that contains amorphous and crystalline phases, with the latter ideally being long-range connected and a dopant that localizes preferentially in the amorphous phase. If these conditions are met, the former—as known from the field of organic photovoltaics for aggregation effects—leads to an offset in the HOMO and LUMO levels between the respective phases, with the phases with the higher order having a smaller band gap (see [Fig. 3(a)]). As a consequence, mobile charge carriers energetically favor to migrate from the amorphous to the crystalline phase, while the dopant counterions remain in the amorphous phase. The transport then takes place mainly in the crystalline phase, which is expected to have higher mobility due to its higher order that remains unaltered as the dopants are incorporated in the

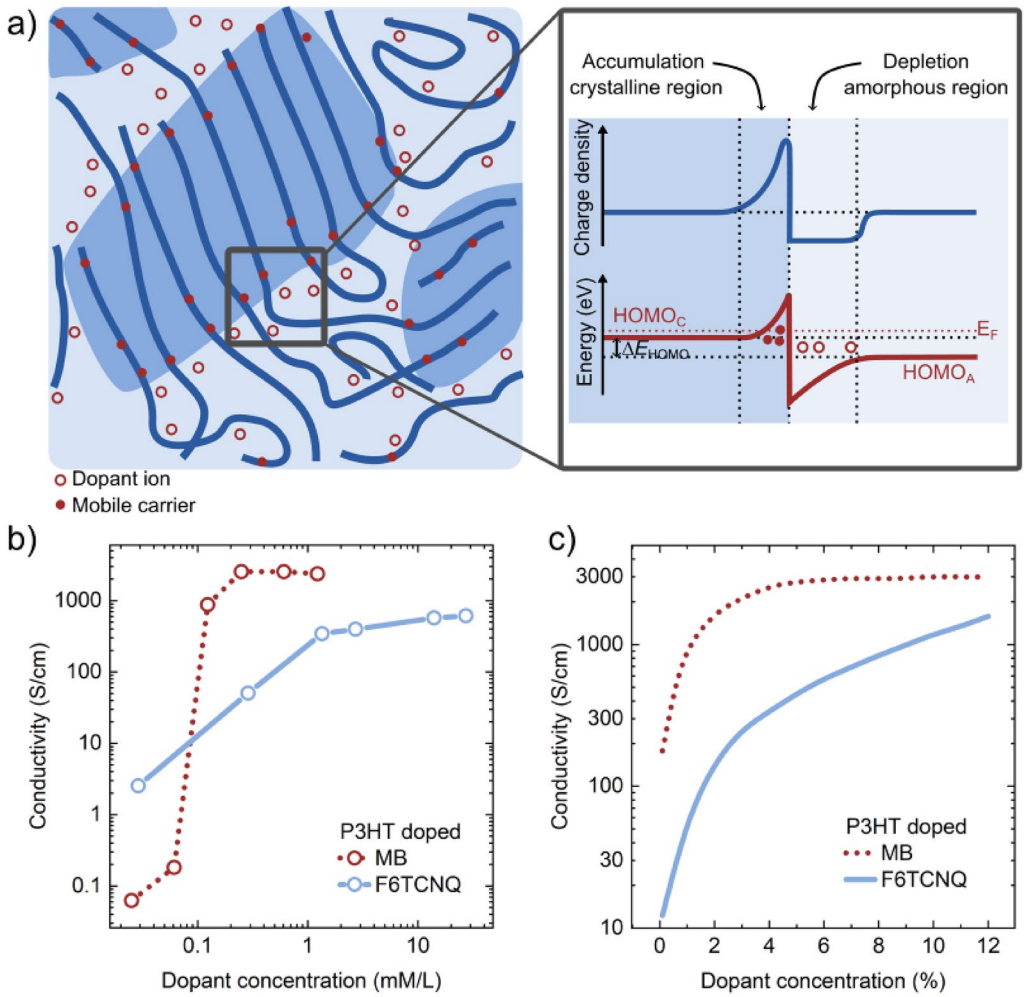

Figure 3: (a) Schematic illustrating the spontaneous modulation doping mechanism in inhomogeneous polymer semiconductors (dark lines), consisting of more (dark colored)- and less (light colored)-ordered regions, with the latter having a larger bandgap, leading to a HOMO level offset as shown on the right. When the dopant (open circles) is preferentially incorporated in the less-ordered regions, mobile charges (closed circles) will transfer to the more-ordered regions, leading to space-charge regions and band bending as shown on the right. (b) Experiment and (c) kMC simulation results for the conductivity of P3HT doped by Magic Blue and F_6TCNQ vs. dopant concentration in the doping solution.

amorphous phase. In addition, the spatial separation between the mobile charge carriers and their static counter charges leads to a significantly reduced Coulomb scattering. Importantly, the process is self-limiting: the migration of mobile charge carriers leads to a space-charge region at the interface between the two phases, resulting in band bending such that the corresponding electric field drives the charge carriers back toward the ions. As a consequence, the migration of mobile charge carriers stops at the moment when the energy required to overcome the resulting potential barrier is larger than the energy gain due to the band offset, see [Fig. 3(a)] (right).

In Ref. [35], this concept of phase-selective doping was implemented into a numerically exact kinetic Monte Carlo simulation based on variable range hopping in a Gaussian Density of States. In addition, the model was extended by a three-phase model for a drying polymer leading to more realistic morphologies. The results [Fig. 3(c)] semi-quantitatively replicate experiments [Fig. 3(b)] on polymers with different morphologies, namely P3HT (semi-crystalline) and PBTTT (liquid crystalline) and suitable dopants, demonstrating the high practical relevance of this concept. Indeed, both polymers show a steep increase in conductivity and a rapid saturation of conductivity when doped with the dopant that localizes in the amorphous phase (here Magic Blue, MB), while the dopant that preferentially sits in the ordered domains (here F_6TCNQ) leads to a significantly weaker increase in conductivity and shows no saturation, see [Fig. 3(b, c)]).

A possible reason for preferential doping of the amorphous phase is a significant higher void density in the amorphous phase as shown by a three-phase model for a drying polymer. The selective positioning of a specific dopant can be understood through two competing factors. First, a steric preference for the

amorphous phase due to a higher void density in the said phase and second a stabilization of diffusing dopants by integer charge transfer (ICT), depending on their location. While the former factor is relevant for all dopants and would lead to the desired modulation doping effect, the latter factor depends on the driving force for ICT of the specific dopant/polymer phase. In the case of F_6TCNQ, which does not dope the amorphous phases of P3HT and PBTTT, it causes the dopant to eventually be incorporated in the more-ordered phase, despite the lower void density, due to the stabilization by ICT [35].

Finally, it should be remarked that the spontaneous modulation doping effect should be active for all material combinations fulfilling the mentioned conditions. However, it has so far only been experimentally demonstrated for rubbing-aligned thin films [35].

Example 2: Dopant alignment

Inspired by the performance increases induced by unidirectional alignment of the polymer backbone, one might wonder whether a similar 1D-like organization of dopant molecules could have a similar effect on the thermoelectric FoM. Although this may sound near-impossible to realize, the incorporation of dopant molecules in quasi-1D strands may actually occur spontaneously. In Ref. [36], Persson et al. used 3D electron tomography to visualize individual Mo(tfd-$COCF_3$)$_3$ dopants in a glycolated polythiophene (p($g_4$2T–T)) matrix and found, at higher loading levels, the dopants to organize in elongated clusters parallel to the surface normal.

In order to test the above idea, we incorporated a modified version of the cellular automaton model from Peumans and Forrest into our kinetic Monte Carlo (kMC) simulator for hopping transport in disordered media [37]. In short, the model works on a grid of 'molecules' that interact through interfacial energies that are typically different for different material combinations. For a 2-component system that leads to 3 energies, $E_{11}, E_{22}, E_{12} = E_{21}$. For a cubic lattice with nearest neighbor interaction, the total system energy becomes

$$E = \frac{1}{2}\sum_{i=1}^{N}\sum_{j=1}^{6}\alpha_{ij}E_{M(i)M(j)} \tag{1}$$

where $M(i) = 1, 2$ is the material of site i and α_{ij} is an anisotropy factor that depends on the relative (x, y, z) orientation of the neighboring sites i and j. The exchange rate of a given pair of sites is then

$$\gamma = \gamma_0 \exp\left(\frac{E - E'}{2k_B T}\right) \tag{2}$$

where E and E' are the energies of the configurations before and after the swap, γ_0 is an attempt frequency, and the factor 2 is there to fulfill detailed balance. The idea is illustrated in [Fig. 4(a)]. Hence, when $E_{11}, E_{22} < E_{12}$, the system will show phase separation by reducing the interfacial area.

Equations (1) and (2) are incorporated in a simple kinetic Monte Carlo program that allow to progress a, typically random, starting situation in time. Typical results are shown in [Fig. 4(b)–(d)]. As in the original work by Peumans and Forrest, running the isotropic system from a random starting configuration (panel b) leads to isotropic clusters that grow in time, see panel c [37]. For enhanced interaction along the z-direction, the clusters become elongated along z, in pleasing agreement with the experiments in Ref. [36], see panel d. For a reduced interaction along z, the clusters become flake like in the x, y-plane, not shown. Despite the phenomenological similarity to the experimental observations, the model does not explain the physical reason for the anisotropic interaction; a discussion thereof is beyond our current purposes.

Running kMC simulations on morphologies as in Fig. 4 leads, for very standard hopping parameters, to the conductivities indicated by the arrows. As anticipated, the conductivity becomes anisotropic in the case of anisotropic dopant clustering, panel d, with an anisotropy factor ~ 2 and highest conductivity along the clustering direction. More surprising are the differences with the isotropic systems. On the one hand, having isotropic clusters (panel c) gives rise to poorer charge transport in all directions. On the other hand, random, molecularly dispersed dopant distributions (panel b) lead to significantly higher conductivities in all directions. At the same time, the finding that having fewer but larger dopant clusters, panel c vs b, hampers conductivity may appear intuitive and in line with experiments that generally show that dopant aggregation is detrimental. Note, however, that in the current simulations, indirect factors like disturbed morphologies are not present, and the effects entirely stem from Coulomb interactions between dopants and mobile charges.

While the above shows that dopant ordering can have significant and measurable effects on charge transport, we must stress that these simulations are far from exhaustive and that results are prone to differ for other parameters, concentrations, etc. As such, this may also form a worthwhile direction of future research.

Summary and outlook

In the first part of this perspective, we have performed a meta-analysis of reported Figures of Merit of organic thermoelectric materials. Overall, we observed an almost complete absence of systematic improvement with time, despite a strongly growing number of publications per year dedicated to the topic matter. In the second part, we addressed possible causes and mitigation strategies. The aggregate data from literature

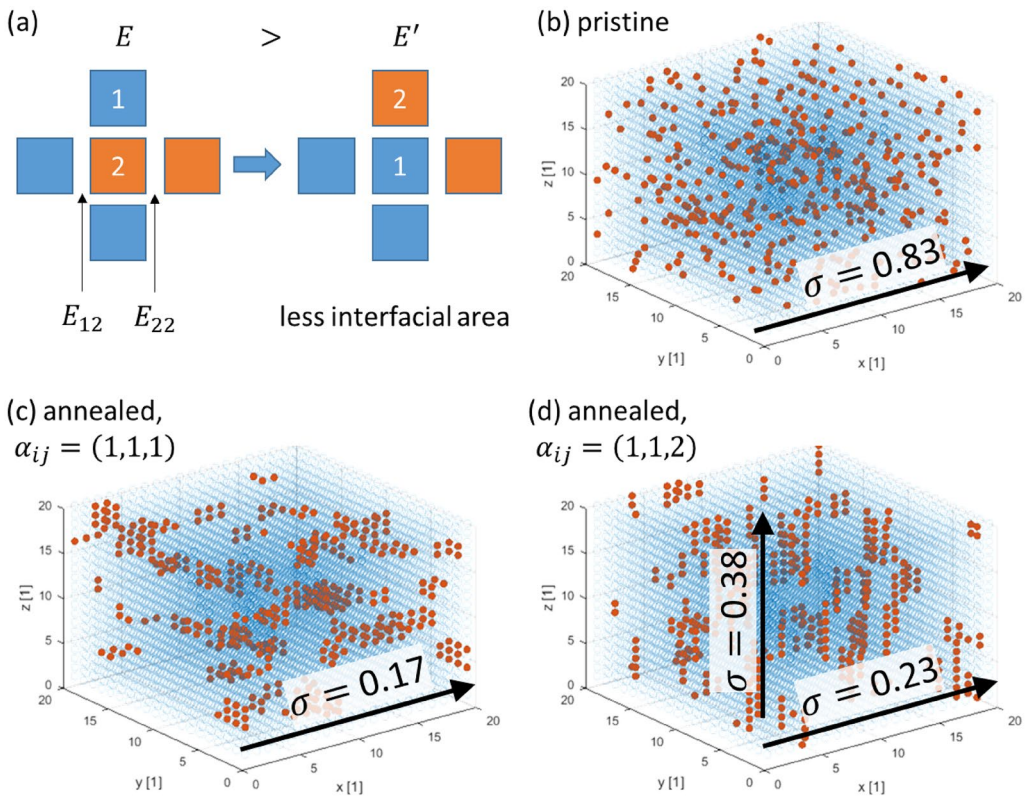

Figure 4: (a) Illustration of the cellular automaton model acting on a small cluster consisting of 2 different molecular species (blue and orange squares). Swapping the molecules marked 1 and 2 reduces the total system energy when $E_{11}, E_{22} < E_{12}$ by reducing the interfacial area. (b–d) typical results of numerical annealing using the cellular automaton model on a 20^3 box with 5% doping (red dots) after 2×10^4 time steps ($E_{11} = E_{22} = 60$ kJ/mol, $E_{12} = 120$ kJ/mol, $T = 450$ K). Host molecules are shown by transparent blue circles. Arrows indicate Ohmic conductivity values in arbitrary units averaged over many configurations (Gaussian disorder $\sigma_{DOS} = 60$ meV, lattice constant $a_{NN} = 1.8$ nm, dielectric constant $\varepsilon_r = 3.6$). For homogeneous systems (b, c) only on direction is shown; for (d), *x* and *y* directions are equivalent.

suggest that it may be hard to significantly improve on current best conductivities of around 1000 S/cm, which implies one would have to beat the trade-off with the Seebeck coefficient or the electronic contribution to the thermal conductivity. Alternatively, and essentially unexplored, is optimizing the (unknown) relation between electronic properties (σ, S, κ_{el}) and the lattice thermal conductivity (κ_{latt}) that seems to dominate the overall thermal conductivity in organic thermoelectric materials.

In this context, it is interesting to compare to the inorganic state-of-the-art that show $zT > 2$ despite a modest conductivity ~ 100 S/cm and a thermal conductivity around 0.3 W/mK that is comparable to organics due to a comparatively high $S >$ 500 µV/K [38, 39]. Here, one has to bear in mind that these records are achieved at $T = 750$–900 K, which is unrealistic for organics. Comparing to Bi_2Te_3, which has zT close to unity around room temperature, paints, however, a similar picture: at an optimal conductivity of ~ 1000 S/cm, Bi_2Te_3 has a comparatively high $S > 250$ µV/K and a modest $\kappa \sim 2$ W/mK [40]. Although the heat and charge transport physics in inorganics differ strongly from organics, the comparison seems to confirm further improvements of organic thermoelectrics are to be sought in S and κ, rather than in σ.

Two approaches, both based on the spatial control of dopant position by bottom-up means are discussed in some quantitative detail in the second part of this perspective. While these examples exploit microscopic inhomogeneities, also more macroscopic inhomogeneity, e.g., in the form of dopant gradients, as recently proposed as a method to improve thermoelectric performance [41, 42], might be worthwhile to pursue. Finally, we should reiterate that the FoM as discussed herein are by no means all that matters for actual applications. For instance, a promising and unconventional direction to solve the crucial issue of (dopant) stability is the use of all-polymer donor–acceptor heterojunctions in which suitably matched polymers act as mutual dopants [43].

Acknowledgments

This work is financially supported by the European Commission through the Marie Sklodowska-Curie project HORATES (GA-955837). M.K. thanks the Carl Zeiss Foundation for

financial support. We are grateful to Gustav Persson, Eva Olsson, Christian Müller, Mariano Campoy, and Mario Caironi for stimulating discussions and (C.M., M.C., and M.C.) for critical reading of the manuscript and to all early stage researchers in the HORATES consortium for assembling the literature data used herein.

Funding

Open Access funding enabled and organized by Projekt DEAL.

Data availability

The authors declare that the data supporting the findings of this study are available within the paper and its supplementary information files.

Declarations

Conflict of interest On behalf of all authors, the corresponding author states that there is no conflict of interest.

Supplementary Information

The online version contains supplementary material available at https://doi.org/10.1557/s43578-024-01321-9.

Open Access

References

1. J. Rivnay, H. Wang, L. Fenno, K. Deisseroth, G.G. Malliaras, Next-generation probes, particles, and proteins for neural interfacing. Sci. Adv. **3**(6), e1601649 (2017). https://doi.org/10.1126/sciadv.1601649
2. K. Walzer, B. Maennig, M. Pfeiffer, K. Leo, Highly efficient organic devices based on electrically doped transport layers. Chem. Rev. **107**(4), 1233–1271 (2007). https://doi.org/10.1021/cr050156n
3. A.D. Scaccabarozzi, A. Basu, F. Aniés, J. Liu, O. Zapata-Arteaga, R. Warren, Y. Firdaus, M.I. Nugraha, Y. Lin, M. Campoy-Quiles, N. Koch, C. Müller, L. Tsetseris, M. Heeney, T.D. Anthopoulos, Doping approaches for organic semiconductors. Chem. Rev. **122**(4), 4420–4492 (2022). https://doi.org/10.1021/acs.chemrev.1c00581
4. HORATES_ITN. Database of Thermoelectric Data for Organic P- and n-Type Materials, 2024. https://doi.org/10.5281/zenodo.10629203.
5. T. Upreti, Y. Wang, F. Gao, M. Kemerink, On the device physics of high-efficiency ternary solar cells. Solar RRL **6**(11), 2200450 (2022). https://doi.org/10.1002/solr.202200450
6. A. Shakouri, Recent developments in semiconductor thermoelectric physics and materials. Annu. Rev. Mater. Res. **41**(1), 399–431 (2011). https://doi.org/10.1146/annurev-matsci-062910-100445
7. S. Scheunemann, M. Kemerink, Thermoelectric properties of doped organic semiconductors. in *Organic Flexible Electronics*; *Woodhead Publishing Series in Electronic and Optical Materials* (Elsevier, Amsterdam, 2021), pp. 165–198.
8. D. Scheunemann, M. Kemerink, Non-Wiedemann-Franz behavior of the thermal conductivity of organic semiconductors. Phys. Rev. B **101**(7), 075206 (2020). https://doi.org/10.1103/PhysRevB.101.075206
9. H. Tang, Y. Liang, C. Liu, Z. Hu, Y. Deng, H. Guo, Z. Yu, A. Song, H. Zhao, D. Zhao, Y. Zhang, X. Guo, J. Pei, Y. Ma, Y. Cao, F. Huang, A solution-processed n-type conducting polymer with ultrahigh conductivity. Nature **611**(7935), 271–277 (2022). https://doi.org/10.1038/s41586-022-05295-8
10. Z. Fan, P. Li, D. Du, J. Ouyang, Significantly enhanced thermoelectric properties of PEDOT:PSS films through sequential post-treatments with common acids and bases. Adv. Energy Mater. **7**(8), 1602116 (2017). https://doi.org/10.1002/aenm.201602116
11. A similar argument can be made about the period 2004–2009 when a similar PCE plateau (at 4–5%) occurred, which was overcome by the advent of donor-acceptor co-polymers that allowed a much greater freedom of design in terms of energy levels and spectral overlap.
12. R.A.J. Janssen, J. Nelson, Factors limiting device efficiency in organic photovoltaics. Adv. Mater. **25**(13), 1847–1858 (2013). https://doi.org/10.1002/adma.201202873
13. A. Polman, M. Knight, E.C. Garnett, B. Ehrler, W.C. Sinke, Photovoltaic materials: present efficiencies and future challenges. Science **352**(6283), aad4424 (2016). https://doi.org/10.1126/science.aad4424
14. B. Ehrler, E. Alarcón-Lladó, S.W. Tabernig, T. Veeken, E.C. Garnett, A. Polman, Photovoltaics reaching for the Shockley-Queisser limit. ACS Energy Lett. **5**(9), 3029–3033 (2020). https://doi.org/10.1021/acsenergylett.0c01790

15. As compared to the hardly absorbing fullerene acceptors, NFA allowed to improve the spectral overlap with the solar spectrum. Simultaneously, a better control over energy level offsets reduced energy/voltage losses.
16. J. Liu, B. van der Zee, R. Alessandri, S. Sami, J. Dong, M.I. Nugraha, A.J. Barker, S. Rousseva, L. Qiu, X. Qiu, N. Klasen, R.C. Chiechi, D. Baran, M. Caironi, T.D. Anthopoulos, G. Portale, R.W.A. Havenith, S.J. Marrink, J.C. Hummelen, L.J.A. Koster, N-type organic thermoelectrics: demonstration of ZT > 0.3. Nat. Commun. **11**(1), 5694 (2020). https://doi.org/10.1038/s41467-020-19537-8
17. A. Dash, D. Scheunemann, M. Kemerink, Comprehensive model for the thermoelectric properties of two-dimensional carbon nanotube networks. Phys. Rev. Appl. **18**(6), 064022 (2022). https://doi.org/10.1103/PhysRevApplied.18.064022
18. I. Zozoulenko, A. Singh, S.K. Singh, V. Gueskine, X. Crispin, M. Berggren, Polarons, bipolarons, and absorption spectroscopy of PEDOT. ACS Appl. Polym. Mater. **1**(1), 83–94 (2019). https://doi.org/10.1021/acsapm.8b00061
19. E.C. Wu, C.Z. Salamat, O.L. Ruiz, T. Qu, A. Kim, S.H. Tolbert, B.J. Schwartz, Counterion control and the spectral signatures of polarons, coupled polarons, and bipolarons in doped P3HT films. Adv. Func. Mater. **33**(19), 2213652 (2023). https://doi.org/10.1002/adfm.202213652
20. V. Untilova, H. Zeng, P. Durand, L. Herrmann, N. Leclerc, M. Brinkmann, Intercalation and ordering of F6TCNNQ and F4TCNQ dopants in regioregular Poly(3-Hexylthiophene) crystals: impact on anisotropic thermoelectric properties of oriented thin films. Macromolecules **54**(13), 6073–6084 (2021). https://doi.org/10.1021/acs.macromol.1c00554
21. D. Scheunemann, E. Järsvall, J. Liu, D. Beretta, S. Fabiano, M. Caironi, M. Kemerink, C. Müller, Charge transport in doped conjugated polymers for organic thermoelectrics. Chem. Phys. Rev. **3**(2), 021309 (2022). https://doi.org/10.1063/5.0080820
22. D. Di Nuzzo, C. Fontanesi, R. Jones, S. Allard, I. Dumsch, U. Scherf, E. von Hauff, S. Schumacher, E. Da Como, How intermolecular geometrical disorder affects the molecular doping of donor-acceptor copolymers. Nat. Commun. **6**, 6460 (2015). https://doi.org/10.1038/ncomms7460
23. M. Duhandžić, M. Lu-Dìaz, S. Samanta, D. Venkataraman, Z. Akšamija, Carrier screening controls transport in conjugated polymers at high doping concentrations. Phys. Rev. Lett. **131**(24), 248101 (2023). https://doi.org/10.1103/PhysRevLett.131.248101
24. I. Salzmann, G. Heimel, M. Oehzelt, S. Winkler, N. Koch, Molecular electrical doping of organic semiconductors: fundamental mechanisms and emerging dopant design rules. Acc. Chem. Res. **49**(3), 370–378 (2016). https://doi.org/10.1021/acs.accounts.5b00438
25. J. Sun, M.-L. Yeh, B.J. Jung, B. Zhang, J. Feser, A. Majumdar, H.E. Katz, Simultaneous increase in seebeck coefficient and conductivity in a doped poly(Alkylthiophene) blend with defined density of states. Macromolecules **43**(6), 2897–2903 (2010). https://doi.org/10.1021/ma902467k
26. G. Zuo, H. Abdalla, M. Kemerink, Conjugated polymer blends for organic thermoelectrics. Adv. Electron. Mater. **5**(11), 1800821 (2019). https://doi.org/10.1002/aelm.201800821
27. A. Abtahi, S. Johnson, S.M. Park, X. Luo, Z. Liang, J. Mei, K.R. Graham, Designing π-conjugated polymer blends with improved thermoelectric power factors. J. Mater. Chem. A **7**(34), 19774–19785 (2019). https://doi.org/10.1039/C9TA07464C
28. O. Zapata-Arteaga, S. Marina, G. Zuo, K. Xu, B. Dörling, L.A. Pérez, J.S. Reparaz, J. Martín, M. Kemerink, M. Campoy-Quiles, Design rules for polymer blends with high thermoelectric performance. Adv. Energy Mater. **12**(19), 2104076 (2022). https://doi.org/10.1002/aenm.202104076
29. H. Thierschmann, R. Sánchez, B. Sothmann, F. Arnold, C. Heyn, W. Hansen, H. Buhmann, L.W. Molenkamp, Three-terminal energy harvester with coupled quantum dots. Nat Nano **10**(10), 854–858 (2015). https://doi.org/10.1038/nnano.2015.176
30. J. Hynynen, E. Järsvall, R. Kroon, Y. Zhang, S. Barlow, S.R. Marder, M. Kemerink, A. Lund, C. Müller, Enhanced thermoelectric power factor of tensile drawn Poly(3-Hexylthiophene). ACS Macro Lett. **8**(1), 70–76 (2019). https://doi.org/10.1021/acsmacrolett.8b00820
31. A. Hamidi-Sakr, L. Biniek, J.-L. Bantignies, D. Maurin, L. Herrmann, N. Leclerc, P. Lévêque, V. Vijayakumar, N. Zimmermann, M. Brinkmann, A versatile method to fabricate highly in-plane aligned conducting polymer films with anisotropic charge transport and thermoelectric properties: the key role of alkyl side chain layers on the doping mechanism. Adv. Funct. Mater. (2017). https://doi.org/10.1002/adfm.201700173
32. R. Sarabia-Riquelme, R. Andrews, J.E. Anthony, M.C. Weisenberger, Highly conductive wet-spun PEDOT:PSS fibers for applications in electronic textiles. J. Mater. Chem. C **8**(33), 11618–11630 (2020). https://doi.org/10.1039/D0TC02558E
33. V. Vijayakumar, Y. Zhong, V. Untilova, M. Bahri, L. Herrmann, L. Biniek, N. Leclerc, M. Brinkmann, Bringing conducting polymers to high order: toward conductivities beyond 105 S Cm−1 and thermoelectric power factors of 2 mW M−1 K−2. Adv. Energy Mater. **9**(24), 1900266 (2019). https://doi.org/10.1002/aenm.201900266
34. D. Scheunemann, V. Vijayakumar, H. Zeng, P. Durand, N. Leclerc, M. Brinkmann, M. Kemerink, Rubbing and drawing: generic ways to improve the thermoelectric power factor of organic semiconductors? Adv. Electron. Mater. **6**(8), 2000218 (2020). https://doi.org/10.1002/aelm.202000218
35. A. Dash, S. Guchait, D. Scheunemann, V. Vijayakumar, N. Leclerc, M. Brinkmann, M. Kemerink, Spontaneous modulation doping in semi-crystalline conjugated polymers leads to high conductivity at low doping concentration. Adv. Mater. (2023). https://doi.org/10.1002/adma.202311303
36. G. Persson, E. Järsvall, M. Röding, R. Kroon, Y. Zhang, S. Barlow, S.R. Marder, C. Müller, E. Olsson, Visualisation of individual

dopants in a conjugated polymer: sub-nanometre 3D spatial distribution and correlation with electrical properties. Nanoscale **14**(41), 15404–15413 (2022). https://doi.org/10.1039/D2NR03554E

37. P. Peumans, S. Uchida, S.R. Forrest, Efficient bulk heterojunction photovoltaic cells using small-molecular-weight organic thin films. Nature **425**(6954), 158–162 (2003). https://doi.org/10.1038/nature01949
38. L.-D. Zhao, S.-H. Lo, Y. Zhang, H. Sun, G. Tan, C. Uher, C. Wolverton, V.P. Dravid, M.G. Kanatzidis, Ultralow thermal conductivity and high thermoelectric figure of merit in SnSe crystals. Nature **508**(7496), 373–377 (2014). https://doi.org/10.1038/nature13184
39. C. Zhou, Y.K. Lee, Y. Yu, S. Byun, Z.-Z. Luo, H. Lee, B. Ge, Y.-L. Lee, X. Chen, J.Y. Lee, O. Cojocaru-Mirédin, H. Chang, J. Im, S.-P. Cho, M. Wuttig, V.P. Dravid, M.G. Kanatzidis, I. Chung, Polycrystalline SnSe with a thermoelectric figure of merit greater than the single crystal. Nat. Mater. **20**(10), 1378–1384 (2021). https://doi.org/10.1038/s41563-021-01064-6
40. I.T. Witting, T.C. Chasapis, F. Ricci, M. Peters, N.A. Heinz, G. Hautier, G.J. Snyder, The thermoelectric properties of bismuth telluride. Adv. Electron. Mater. **5**(6), 1800904 (2019). https://doi.org/10.1002/aelm.201800904
41. T. Ma, W. Kent, B.X. Dong, G.L. Grocke, S.N. Patel, Continuously graded doped semiconducting polymers enhance thermoelectric cooling. Appl. Phys. Lett. **119**(1), 013902 (2021). https://doi.org/10.1063/5.0055634
42. J. Liu, M. Craighero, V.K. Gupta, D. Scheunemann, S.H.K. Paleti, E. Järsvall, Y. Kim, K. Xu, J.S. Reparaz, L.J.A. Koster, M. Campoy-Quiles, M. Kemerink, A. Martinelli, C. Müller, Electrically programmed doping gradients optimize the thermoelectric power factor of a conjugated polymer. Adv. Funct. Mater. (2024). https://doi.org/10.1002/adfm.202312549
43. K. Xu, H. Sun, T.-P. Ruoko, G. Wang, R. Kroon, N.B. Kolhe, Y. Puttisong, X. Liu, D. Fazzi, K. Shibata, C.-Y. Yang, N. Sun, G. Persson, A.B. Yankovich, E. Olsson, H. Yoshida, W.M. Chen, M. Fahlman, M. Kemerink, S.A. Jenekhe, C. Müller, M. Berggren, S. Fabiano, Ground-state electron transfer in all-polymer donor-acceptor heterojunctions. Nat. Mater. **19**, 738–744 (2020). https://doi.org/10.1038/s41563-020-0618-7